Structural Eng. / Earthquake Eng. Vol. 6. No. 2, 239s-250s. October 1989
Japan Society of Civil Engineers (Proc. of JSCE No. 410/I-12)

A NEW FORMULA TO PREDICT THE ULTIMATE SHEAR STRENGTH OF A PLATE GIRDER

By Shigeru KURANISHI, Masatoshi NAKAZAWA** and Tetsuo IWAKUMA****

In this paper, a new formula to predict the ultimate shear strength of a plate girder is proposed on the basis of the numerical analysis. The analysis of an end panel isolated from the whole structure can describe the stress distribution in the shear panel sufficiently. A stress distribution model in the ultimate state is constructed by generalization of the numerical results. In order to show its validity, the predicted strength by the proposed formula is compared with those by Basler and Rockey et al., and also with the available experimental data.

Keywords: plate girder, shear strength, tension field, ultimate strength analysis

1. INTRODUCTION

On the ultimate shear strength of a plate girder, many researchers have been studying the formation of the tension field and the post-buckling strength by the experimental or theoretical approaches[1)-14)]. These studies have shown that the strength of a shear panel is generally affected by the shear elastic buckling strength, the post-buckling strength due to the formation of the tension field, and the stiffness contribution by the flange plates and stiffeners surrounding the web plate.

Basler[1)] did not include the anchor action by the flanges, and assumed the constant tensile stress in a band in addition to the uniform shearing stress at the buckling load. This band is formed obliquely in the web plate between the transverse stiffeners. The ultimate state is reached when the yield condition is satisfied by the uniform shearing stress and tensile stress in this band. It was pointed out firstly by Gaylord[2)] and later by Fujii[3)] that the original model of Basler does not satisfy the equilibrium condition of forces. The modified Basler's equation corrected is also presented but yields the inferior accuracy. Hasegawa, Nishino and Okumura[4)] introduced the flange force in order to satisfy the equilibrium condition of a whole system, and pointed out that the final expression itself is not necessary to be modified. On the other hand, Rockey and Skaloud[5)] and Porter, Rockey and Evans[6)] assumed the stress distribution taking account of the anchor action by the flanges which had been observed in their experiments. In Ref. 7) by Rockey, Evans and Porter, the inclination of the tension field band is approximately two thirds of that of the diagonal of the web plate, and its width depends on the location of a plastic hinge in the flange. In these proposed collapse models, the stress field assumed is discontinuous across the sides of the tension field

* Member of JSCE, Dr. Eng., Professor, Department of Civil Engineering, Tohoku University (Aoba Sendai 980 JAPAN).
** Member of JSCE, M. Eng., Research Associate, Department of Civil Engineering, Tohoku University.
*** Member of JSCE, Ph. D., Associate Professor, Department of Civil Engineering, Tohoku University.

band, and the inclination of the tensile principal direction is constant in the tension field. Moreover, the total shear force varies with the location of the cross section on which it is calculated in the model of Ref. 7), which will be henceforth called Rockey et al.'s model.

Recently Marsh[12] proposed a new simple formula in terms of the pure shear elastic buckling stress on the basis of his stress distribution model for a web plate subjected to pure shear forces. However, in the similar manner as Rockey et al. have done, the plastic hinges in the flanges are also assumed to finally cause the panel to fail. Thus the ultimate shear strength is calculated as the total resisting capacities of the web and flanges.

Although there are proposed many ideas with respect to the configuration of the tension field and/or the collapse model, no widely accepted shear strength formula is established yet. A few studies[11),13] have been made by the numerical approach, but their purposes are not directly related to the proposal of the design formula.

In this paper, the stress distribution of the panel in the ultimate state is investigated by the elastic-plastic finite element analysis[13]. A stress distribution model is derived from examination of the stress state in the ultimate state, and a new formula to predict the shear strength is proposed. Then, the ultimate strength given by this formula is compared with that by the numerical analysis. Finally, the correlation analysis is carried out between the predicted ultimate strength, those by Basler or Rockey et al. and the experiments.

2. CHARACTERISTICS OF TENSION FIELD AND STRESS DISTRIBUTION

In general, the stress state of the shear panel is almost uniform and in pure shear before buckling, but after that, the tensile stresses in the diagonal direction of the web plate becomes significant, and then the tension field is formed. The numerical study of the Model I in Ref. 13) deals with a web plate with the upper and lower flanges connected. The transverse stiffener sides of the panel are simply supported in the out-of-plane direction and the in-plane longitudinal displacement is fixed along these sides. The results show that the inclination of the tension field band from the horizontal line becomes a little flatter than that of the diagonal of the panel. The partial anchor action by the flanges is recognized unlike the assumption of Basler, and the configuration of the tension field becomes rather similar to the one by Porter, Rockey and Evans[6]. The yielded zones develop in a diagonally directed band and eventually lead to the formation of collapse mechanism, but the plastic hinges do not appear in the flanges. The larger the aspect ratio α of the web plate becomes, the narrower the width of the tension field becomes, and the flatter the inclination of the tensile principal direction becomes. When the depth-thickness ratio β is small, the ultimate state is achieved relatively sooner after buckling by the full yielding, and the stress state is almost the same as that in the buckled state; i. e. in pure shear. Hence both the compressive and tensile stresses are large, and the tension field does not develop so clearly as a band. When the flange rigidity is decreased, the anchor action by the flanges becomes insignificant and the width of the tension field becomes narrower. In this case, the inclination of the tensile principal stresses tends to increase to become almost parallel to the diagonal of the panel.

Fig. 1 shows the stress distributions on the typical surfaces of a panel in the ultimate state when the depth-thickness ratio $\beta=250$ and the aspect ratio $\alpha=0.75$, 1.0 or 1.5, where τ_Y denotes the shear yield stress. The tensile stress σ_t on AA′ takes relatively higher value in the neighborhood of the diagonal line BB′, which indicates the formation of the tension field. On the contrary, the compressive stresses σ_c on BB′ takes a lower value on the other diagonal line AA′. On the other hand, in the vicinity of the corner region near the points B and B′, both the compressive and tensile stresses become large owing to the gusset plate action. Then, from Eq. (2·b), the shearing stress τ_{xy} on AB′ or A′B′ also becomes large in this corner region near B′. The stress components σ_x and σ_y along these lines are smaller than τ_{xy}, and especially the component σ_y is the smallest on all sides and will be set zero in the construction of a model

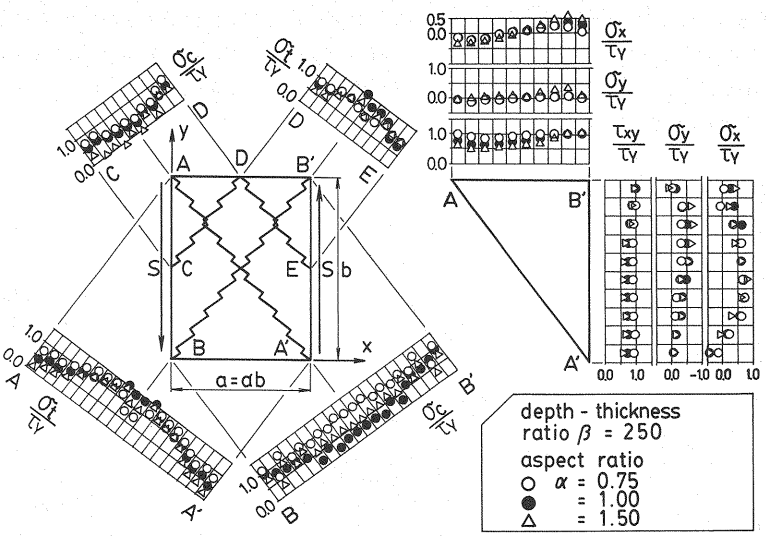

Fig. 1 Numerical evaluation of stresses on typical surfaces of the shear panel in the ultimate state.

later on.

The occurrence of plastic hinges in flanges and the apparent contribution of flange rigidity to the shear strength have not been recognized in our numerical study. Therefore the ultimate shear strength will be estimated by the resisting capacity of the plate only, and is given in terms of its elastic buckling strength. However, the effect of the flange rigidity will be taken into account in evaluating the buckling strength.

3. A NEW FORMULA TO PREDICT THE ULTIMATE SHEAR STRENGTH

(1) A collapse model and a design formula

A collapse model presented here takes into account the following several features referring the results obtained by the numerical analysis carried out previously[13]. The stress of each strip is assumed to be uniform in the strip but the stress level may vary depending on the rigidity of the surrounding members anchoring the strips. The ultimate state is achieved when some of the tension strips in the central part of the panel begin to yield. At this state, the diagonal line BB′ is considered to begin to show significant elongation but plastic hinges are not yet formed in the flanges. Moreover, considering the difficulty of modelling of the stress distribution in the extreme state where plastic hinges are formed, it is straightforward to take the collapse model of web plate separately. Pure shear loading along the four sides of the web plate is adopted to estimate the genuine shear strength. Therefore, the influence of bending moment on the panel is not directly included in this collapse model.

The collapse model is composed of two sets of obliquely placed strips being anchored to the surrounding flexible members as shown in Fig. 2. Each set of strips directed parallel to each diagonal line AA′ or BB′ is mainly subjected to compression or tension respectively.

In order to express a stress distribution from this collapse model, we begin with the following two basic assumptions for the stress components; (i) the tension field forms parallel to the diagonal line BB′, and the tensile stress σ_t is constant along the line parallel to BB′; i.e.

$$\sigma_t = f(\eta - \xi) \quad \cdots\cdots (1\cdot a)$$

where ξ and η are the normalized coordinates defined by $\xi \equiv x/a$ and $\eta \equiv y/b$ respectively, while a and b is the transverse stiffener spacing and the girder depth respectively; (ii) the compressive stress σ_c in the direction parallel to AA′ is also constant in each thin strip in the same direction; i.e.

$$\sigma_c = g(\eta + \xi) \quad \cdots\cdots (1\cdot b)$$

where the stress σ_c is reckoned positive if compressed in the direction of AA′. It should be noted that σ_t and σ_c are not the principal stresses but the contravariant components in the skew coordinate system. θ_d is the angle of the diagonal line BB′ in Fig. 2 and is related to the aspect ratio by $\tan\theta_d=1/\alpha$. Then the coordinate transformation yields

$$\sigma_x=\frac{\sigma_t-\sigma_c}{1+\cos 2\theta_d}-\sigma_y\tan^2\theta_d,\quad \tau_{xy}=\frac{\sigma_t+\sigma_c}{2\sin 2\theta_d} \qquad (2\cdot a, b)$$

For the purpose of constructing a stress distribution model only, we need not to specify other stress components.

Consider that each thinly-sliced strip parallel to AA′ is a pinned column subjected to the compression σ_c, and that all these strips are being buckled simultaneously in the ultimate state. The analogy of the Euler buckling formula implies that σ_c is inversely proportional to the square of each strip length. Therefore, σ_c takes its absolute minimum stress $(\sigma_c)_{\min}$ along the line AA′, and thus Eq. (1·b) can be expressed as

$$\sigma_c=g(\eta+\xi)=\begin{cases}(\sigma_c)_{\min}/(\eta+\xi)^2, & \text{for } 0<\eta+\xi\leqq 1\\ (\sigma_c)_{\min}/\{(\eta-1)+(\xi-1)\}^2, & \text{for } 1\leqq\eta+\xi<2\end{cases} \qquad (3)$$

The minimum value $(\sigma_c)_{\min}$ depends on the aspect ratio α, and is determined from our numerical results explained in the preceding section. The relationship obtained numerically is shown by the open and closed circles in Fig. 3, where τ_{cr} denotes the shear buckling stress of a panel with its four edges simply supported. One of the simple models can be obtained by approximating this relation as

$$\frac{(\sigma_c)_{\min}}{\tau_{cr}}=2\sin^2\theta_d=\frac{2}{1+\alpha^2} \qquad (4)$$

The shear panel considered here is subjected to shear force along the vertical sides, where both σ_x and σ_y are very small compared with τ_{xy} in the ultimate state, as mentioned in the preceding section. Therefore, along the vertical sides, we set σ_x and σ_y zero. Hence follows from Eqs. (2·a) and (1)

$$\sigma_t(\xi=0)=\sigma_c(\xi=0);\ \text{i.e.}\quad f(\eta)=g(\eta) \qquad (5)$$

Therefore, using Eq. (3),

$$\sigma_t=f(\eta-\xi)=\frac{(\sigma_c)_{\min}}{(\eta-\xi)^2} \qquad (6)$$

Substitution of Eqs. (3), (4) and (6) into Eq. (2·b) yields

$$\tau_{xy}=\frac{1}{2}\tau_{cr}\tan\theta_d\left\{\frac{1}{(\eta-\xi)^2}+\frac{1}{(\eta+\xi)^2}\right\},\quad \text{for } 0<\eta+\xi\leqq 1 \qquad (7)$$

However, the yield condition requires Eq. (7) that

$$\tau_{xy}(\xi=0)=\frac{\tau_{cr}\tan\theta_d}{\eta^2}\leqq\tau_Y \qquad (8)$$

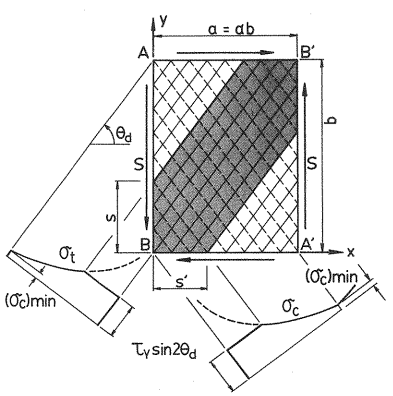

Fig. 2 Collapse model and stress distributions σ_t and σ_c in the strips.

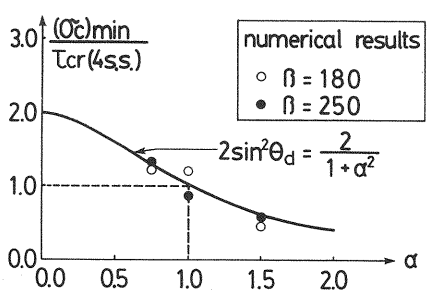

Fig. 3 Relationship between the minimum compressive stress σ_c and aspect ratio α.

because σ_x and σ_y are zero along $\xi=0$. Hence the normalized distances s/b on the η-axis and s'/a on the ξ-axis in which τ_{xy} equals τ_Y in Fig. 2 are obtained from Eq. (8) as

$$s/b=\sqrt{\frac{\tau_{cr}}{\tau_Y}\tan\theta_d}=s'/a \quad \cdots\cdots (9)$$

The width of the tension field band is thus given by $2\,s\cos\theta_d$ or $2\,s'\sin\theta_d$. Although the basic concept for the collapse model is quite different, the gusset plate model[14] has the similar idea for the occurrence of yielding in the corner zone. In this case, the shape of this gusset plate is also presented by Eq. (9) after replacing $\tan\theta_d=1.0$; i.e. θ_d is fixed to be $\pi/2$. Furthermore, substitution of Eqs. (5) and (2·b) into Eq. (8) yields

$$\tau_{xy}(\xi=0)=\frac{\sigma_t(\xi=0)}{\sin 2\theta_d}=\frac{\sigma_c(\xi=0)}{\sin 2\theta_d}\leqq\tau_Y;\ \text{i.e. } \sigma_t(\xi=0)\text{ and }\sigma_c(\xi=0)\leqq\tau_Y\sin 2\theta_d \quad \cdots\cdots (10)$$

The final form of a stress distribution model is shown in Fig. 4.

The total shear force S along the vertical side is obtained by integrating Eq. (7) along $\xi=0$ and considering Eqs. (8) and (9) as

$$S=\tau_Y s t+b t\,\tau_{cr}\tan\theta_d\int_{s/b}^{1}\left(\frac{1}{\eta}\right)^2 d\eta=b t\{2\sqrt{\tau_{cr}\tau_Y\tan\theta_d}-\tau_{cr}\tan\theta_d\}$$

or can be rewritten in the non-dimensional form as

$$\frac{\tau_{ult}}{\tau_Y}\equiv\frac{S}{\tau_Y b t}=2\sqrt{\frac{\tau_{cr}}{\tau_Y}\tan\theta_d}-\frac{\tau_{cr}}{\tau_Y}\tan\theta_d \quad \cdots\cdots (11)$$

where t is the thickness of the web plate. Although this result depends on the choice of Eq. (4) as well as the stress field of Eq. (1), the formula has the simple form and is easy to use. In the case of the square web plate, this formula results in that by Marsh[12].

(2) Shear buckling strength and flange rigidity

For completion of the construction of a model, the shear buckling strength τ_{cr} must be given appropriately. The buckling strength is greatly affected by the boundary conditions, such as the rigidity of flanges and vertical stiffeners, but the conditions specified by each researcher are quite different. For instance, Basler[1] did not expect the contribution of flanges to the buckling strength, and thus all the four edges were simply supported. Although Rockey and Skaloud[5] pointed out that the shear buckling strength depends on the rigidity of the sided members, they employed the simply supported boundary condition for a conservative estimate, because there had not existed enough experimental results yet. On the other hand, Herzog[8] and Niinobe[10] assumed that the web plate was clamped along the flange sides and simply supported

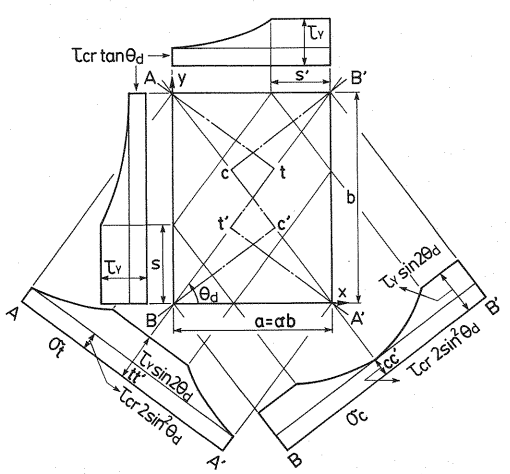

Fig. 4 Stress distributions in a shear collapse model.

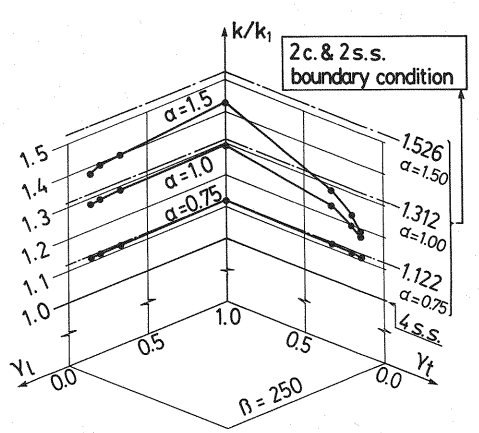

Fig. 5 Effect of flange rigidity on the shear buckling strength.

along the vertical sides.

We here consider that the flange rigidity plays a more important role than the transverse stiffeners, and again investigate the relationship between the shear elastic buckling strength and flange rigidity numerically. In order to take into account only the stiffening effect by the flanges, the vertical edges are simply supported. The mainly used two parameters are the same as those in Ref. 13), which are the reduction ratios of the torsional rigidity γ_t and of the lateral flexural rigidity γ_l of the flange. The initial out-of-plane deflections are introduced by the doubly sinusoidal half wave and the maximum amplitude of it is set one tenth of the thickness, and the buckling load is determined by the $P-\delta^2$ method[15]. Fig. 5 shows the relationship between the flexural or torsional rigidity of flanges and the buckling coefficient k, which is defined as $\tau_{cr}=k\pi^2E/\{12(1-\nu^2)\beta^2\}$, where E and ν are Young's modulus and Poisson's ratio respectively. In the ordinate, k is normalized by the pure shear buckling coefficient of a plate with four edges simply supported, k_1. The torsional rigidity of the flange seems to affect the shear buckling strength more. In the case of $\alpha=0.75$, the buckling coefficient is more or less equal to the one with two edges simply supported and the others clamped. On the other hand, in the case of $\alpha=1.0$ and 1.5, the buckling coefficient becomes smaller as the flange rigidity decreases, and approaches to the one in which four edges are simply supported. The same form by Moriwaki and Fujino[9] is employed to take into account conservatively the influence of the aspect ratio α on the buckling strength, and from Fig. 5, the buckling stress τ_0 can be approximately given by

$$\tau_0=\tau_{cr2}\alpha^{-1/3}(0.10\,\alpha\gamma_0+0.86) \quad (12)$$

where γ_0 takes the smaller value of either unity or the reduction ratio of the torsional rigidity, and is expressed as

$$\gamma_0=\mathrm{MIN}(\gamma_t,\ 1),\ \gamma_t\equiv\frac{b_f t_f^3}{b_{f0}t_{f0}^3} \quad (13)$$

$$b_{f0}=\{t+\sqrt{t^2+8\rho\psi bt}\}/2,\ t_{f0}=\rho\, bt/b_{f0}$$

$$\rho\equiv b_f t_f/bt=0.5,\ \psi\equiv(b_f-t)/2/t_f=13.0$$

where b_f and t_f are the width and thickness of the flange plate, while b_{f0} and t_{f0} are the corresponding reference width and thickness in Ref. 13). ρ is the ratio of cross-sectional area of a flange plate to that of a web, and ψ is the width-thickness ratio of the free width of outstanding part of the flange plate. τ_{cr2} is the shear buckling stress of a plate with flange-sides clamped and vertical-sides simply supported. Let τ_{cr1} denote the shear buckling stress of a plate all-sides simply supported. Then the corresponding buckling coefficients k_1 and k_2 can be approximated respectively as[10]

$$k_1=\begin{cases}5.34/\alpha^2+4.00, & \text{if } \alpha\leqq1.0\\ 4.00/\alpha^2+5.34, & \text{otherwise}\end{cases} \quad (14\cdot a)$$

$$k_2=\begin{cases}5.34/\alpha^2+6.55/\alpha-13.71+14.10\,\alpha, & \text{if } \alpha\leqq1.0\\ 8.98+6.18/\alpha^2-2.88/\alpha^3, & \text{otherwise}\end{cases} \quad (14\cdot b)$$

As is clear from Fig. 5, the conservative estimate of the shear buckling stress must not exceed τ_{cr2} and must not be less than τ_{cr1}. Therefore the final form of the buckling strength which also includes the inelastic effect can be given by

$$\tau_{cr}=\sqrt{\tau_2\,\mathrm{MIN}(\tau_2,\ 0.8\,\tau_Y)} \quad (15)$$

$$\tau_2=\mathrm{MIN}(\tau_1,\ \tau_{cr2}),\ \tau_1=\mathrm{MAX}(\tau_0,\ \tau_{cr1}) \quad (16)$$

where MAX (,) takes the value of the larger one of two arguments. From Eqs. (11) and (12), the effect of the flange rigidity can be included in the estimate of the ultimate shear strength.

4. DISCUSSION

(1) Variation of the present formula

In constructing a stress distribution model, we use an approximated relation Eq. (4) between α and $(\sigma_c)_{\min}$ in Fig. 3. The left-hand side of this Eq. (4) must be 1.0 when $\alpha=1.0$, because (σ_c) must be equal

to τ_{xy} when $\xi-\eta$ coordinates forms an orthogonal system. As is clear from the figure, it is possible to draw any other such curves to fit those data to some extent, and the different forms of the formula may be obtained. However Eq. (4) among those makes the final form of formula the simplest, which is very important from the practical point of view. As an illustration, the discrepancy is shown here when a straight line is chosen instead of Eq. (4). A linear relation based on the least square method is given by

$$\frac{(\sigma_c)_{\min}}{\tau_{cr}}=-0.9832(\alpha-1)+1\simeq-1.0(\alpha-1)+1 \quad \cdots\cdots (17)$$

The final formulae of the ultimate shear strength resulting from those two relations can be given by the same expression as

$$\frac{\tau_{ult}}{\tau_Y}=2\sqrt{\frac{\tau_{cr}}{\tau_Y}\kappa}-\frac{\tau_{cr}}{\tau_Y}\kappa$$

$$\kappa=\begin{cases}1/\alpha=\tan\theta_d, & \text{when Eq. (4) is employed}\\ \dfrac{(\alpha^2+1)(2-\alpha)}{2\alpha}, & \text{when Eq. (17) is employed}\end{cases} \quad \cdots\cdots (18\cdot a, b)$$

The difference between these two formulae is less than 8% in the range of the aspect ratio, $0.6\leqq\alpha\leqq1.5$, as shown in Fig. 6. In the same range of α, the effect of the slope change in the linear relation Eq. (17) is also examined. At most 10% change of the slope leads to the change of the value of τ_{ult}/τ_Y merely within 3.9%. Therefore, the total difference due to the change of functions may be at most about 12%. Although Eq. (17) leads more conservative ultimate strength than the one by employing Eq. (4), it leads wider scattering in the correlation test of later section 4. (5), and can not be applied in the range of $\alpha>2.0$. Several formulations in the hyperbola type are also adopted, but the difference is more or less similar to the one employing Eq. (4). Moreover, the replacement of τ_{cr}(4 s. s.) by τ_{cr} which includes the effect of flange rigidity and inelastic buckling is also not affected significantly to the ultimate shear strength obtained finally. Since the final results are not sensitive to the choice of the function, Eq. (4) is proposed because of its simple form.

(2) Location-dependency of the definition of τ_{ult}

The final formula, Eq. (11), is defined by the total shear stresses integrated along the left- or right-most vertical cross-section of the web plate. As seen in Eq. (7), the shear strength is a function of the longitudinal coordinate ξ of the panel. Consequently, the shear strength may vary according to the cross-section on which it is calculated. Fig. 7 shows the configurations of the yielded band for the typical case of $\beta=250$. The width of the yielded band is determined by the stress distributions of σ_x and τ_{xy} along the line of given ξ by using the von Mises's yield condition. The shear stress distribution inside the yielded band is interpolated linearly in the η directions along the line of certain ξ. Fig. 8 shows the variation of total shear force in the direction of ξ, and the difference becomes largest at the mid-section of the panel ($\xi=0.5$). In some cases, smaller shear force is given but the difference is not so large. The relation between the maximum difference of shear force calculated at the mid-section of the panel and the aspect ratio α is shown in Fig. 9 for the typical values of the depth-thickness ratio β. This figure indicates that the difference is nearly constant for the larger value of α, and the largest difference becomes up to about 30%. Compared with the numerical results, the model presented here is overestimating the shear stress level in the yielded band at the mid-section of a panel.

One of the reasons for this overestimation should come from the presence of the vertical compressive stress σ_y induced by the in-plane deformation as shown in Fig. 4 of Ref. 13) or Ref. 16). When this stress σ_y is introduced, the width of the yielded band is expected to become wider and the shear stress level is decreased, and it can explain the numerical results well. Therefore, in order to construct more suitable stress distributions in the panel, it is necessary to introduce this stress component σ_y into the formulations. However, these expressions will become more complex, and it is less meaningful for the

practical calculation of the ultimate shear strength.

(3) Inclination of the tensile principal direction

Although the tension field is simply assumed to form parallel to the diagonal line BB′ in Fig. 2, the tensile principal direction ϕ varies with the location inside the panel unlike other tension field models. Basler[1] and Rockey et al.[7] assumed ϕ respectively as

$$\phi=\tan^{-1}(\sqrt{\alpha^2+1}-\alpha),\quad \phi\simeq\frac{2}{3}\theta_d=\frac{2}{3}\tan^{-1}\left(\frac{1}{\alpha}\right) \qquad \cdots\cdots (19\cdot a, b)$$

As is observed in the numerical simulation, this inclination becomes smaller than that of the diagonal at the center of the panel, but it becomes nearly 45 degrees in the corner region owing to the gusset plate action. Fig. 10 shows the angle of the tensile principal directions along the diagonal of a panel by the numerical analysis, Basler's model, Rockey et al.'s and the present model. In our model, the angle becomes the smallest at the center of the panel, and the tensile principal direction is given in terms of the normalized distance ζ from the corner by

$$\phi=\begin{cases}\dfrac{1}{2}\tan^{-1}\left\{\dfrac{\alpha+\dfrac{\tau_{cr}}{\tau_Y}\dfrac{1}{4\zeta^2}\alpha}{\alpha-\dfrac{\tau_{cr}}{\tau_Y}\dfrac{1}{4\zeta^2}}\right\}, & \text{for } \zeta_0\leqq\zeta\leqq(1-\zeta_0)\\ \dfrac{\pi}{4}, & \text{for } 0\leqq\zeta<\zeta_0,\ (1-\zeta_0)<\zeta\leqq 1\end{cases} \qquad \cdots\cdots (20)$$

where

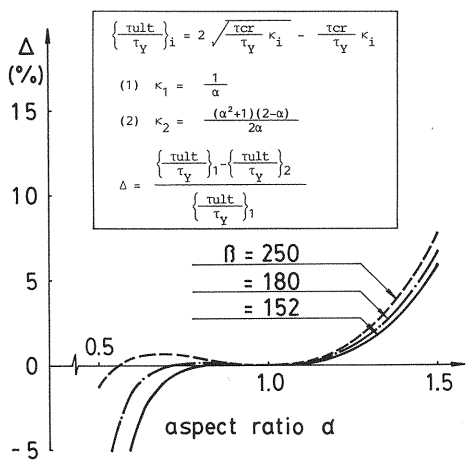

Fig. 6 Difference between Eq. (18·a) and (18·b).

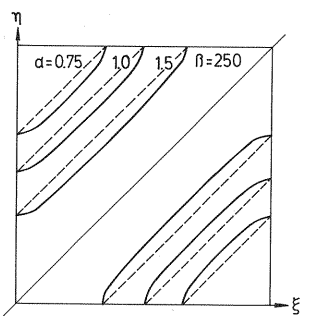

Fig. 7 Configurations of yielded band calculated from the presented stress distributions.

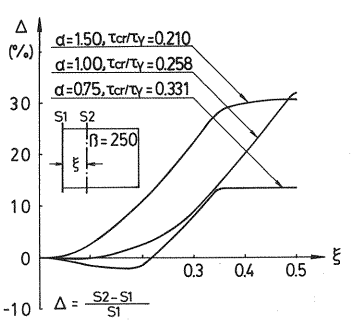

Fig. 8 Variation of total shear force in the longitudinal direction.

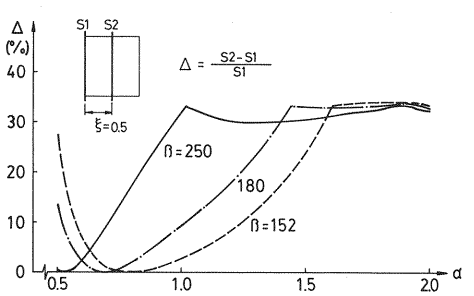

Fig. 9 Difference of total shear force between the left or right-most vertical surface and the mid-section of the panel.

$$\zeta_0=\sqrt{\frac{1}{4\alpha}\frac{\tau_{cr}}{\tau_Y}}=\frac{1}{2}(s/b) \quad (21)$$

Other models in Eq. (19) yield slightly different angles, but they are smaller than the numerical one. Only our model takes the effect of the depth-thickness ratio β and the flange rigidity into account through the computation of τ_{cr}, and reflects the numerical results fairly well. Since ϕ becomes smaller for the large value of α and β and for the small value of γ_t, Eq. (20) represents well the characteristics of ϕ as described in the section 2.

(4) Effect of the bending moment

In our formula for a shear panel, the global stress state is assumed to be in pure shear. However, the end panel of the actual plate girders is also subjected to the applied bending moment.

In order to examine the effect of the bending moment on the shear buckling strength, consider one end panel subjected to both the shear and bending. The interaction formula for the combined buckling stress of bending and shear is given by[17]

$$\left(\frac{\tau'_{cr}}{\tau_{cr}}\right)^2+\left(\frac{\sigma'_{cr}}{\sigma_{cr}}\right)^2=1.0 \quad (22)$$

where τ_{cr} and σ_{cr} are the buckling stresses under pure shear and pure bending respectively, while τ'_{cr} and σ'_{cr} are the corresponding reduced buckling stresses due to coupling. If the shear panel considered is the end panel of a simply supported girder, the bending moment on one side $M=aS$, while it vanishes on the other side. Let Z denote the section modulus of the girder, and $M=Z\,\sigma'_{cr}$ at buckling. Since $S=\tau'_{cr}\,bt$, the stress state of a buckled panel can be approximated as

$$\sigma'_{cr}=\frac{a}{Z}(\tau'_{cr}\,bt) \quad (23)$$

Substituting Eq. (23) into Eq. (22) and solving for τ'_{cr}, we obtain the reduced shear buckling stress with the effect of the bending moment distribution as

$$\frac{\tau'_{cr}}{\tau_Y}=\left\{\left(\frac{\tau_Y}{\tau_{cr}}\right)^2+\left(\frac{abt}{\sqrt{3}\,Z}\frac{\sigma_Y}{\sigma_{cr}}\right)^2\right\}^{-1/2} \quad (24)$$

where the tensile yield stress $\sigma_Y=\sqrt{3}\,\tau_Y$ is introduced. Therefore, after substitution of Eq. (15) into the first term of the right-hand side of Eq. (24), the ultimate shear strength τ_{ult} can be obtained by replacing τ_{cr} in Eq. (11) by τ'_{cr} of Eq. (24). The buckling stress in pure bending σ_{cr} of a plate with four edges simply supported is given by[18]

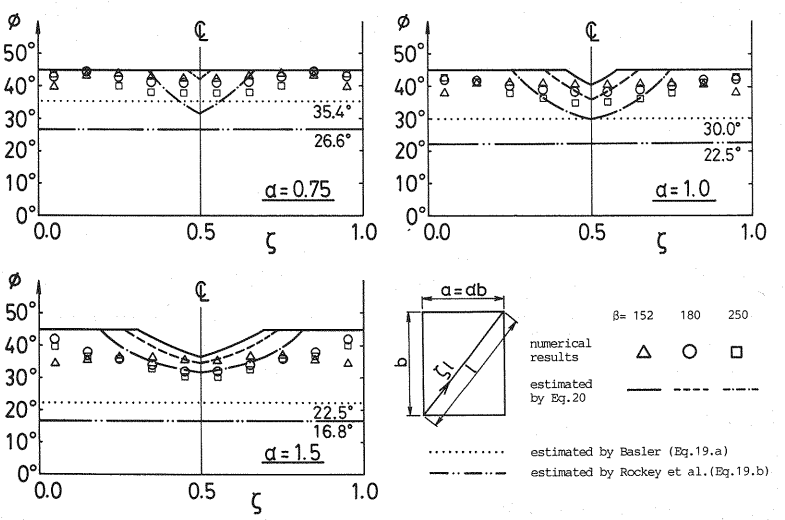

Fig. 10 Tensile principal directions in the tension field.

$$\sigma_{cr}=k_b\frac{\pi^2E}{12(1-\nu^2)}\left(\frac{1}{\beta}\right)^2,$$

$$k_b=\begin{cases}15.87+1.87/\alpha^2+8.6\,\alpha^2, & \text{if } \alpha\leqq 2/3\\ 23.9, & \text{otherwise}\end{cases} \quad \cdots\cdots (25)$$

Since this discussion is restricted to one end panel, it may be rather a underestimation of the effect of bending moment in the case of the intermediate panels.

(5) Comparison between formulae and experimental results

Our formula is compared with that by Basler in Fig. 11, where the numerical results are also shown. Two formulae differ in the range of low buckling strength. This discrepancy stems from the fact that Basler's formula does not include the effect of the depth-thickness ratio, and it tends to give higher strength for the smaller value of τ_{cr}/τ_Y; i. e. for the larger value of β. As long as α is less than 1.0, our formula gives predictions closer to the numerical results. In the case of α being 1.5, this formula gives a little lower strength than the numerical ones, but it is conservative estimation.

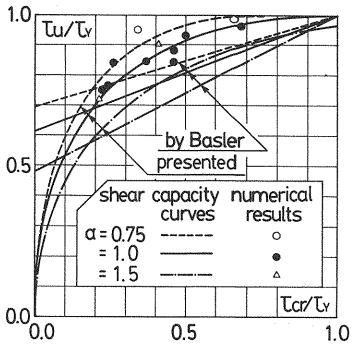

Fig. 11 Comparison between the numerical results and formulae for shear resisting capacity.

Fig. 12 shows the correlation of the strength formulae with the available experimental results[19]. In these figures, n, *mean*, SD and CV denotes the number of samples, the mean value of the ratios of estimated

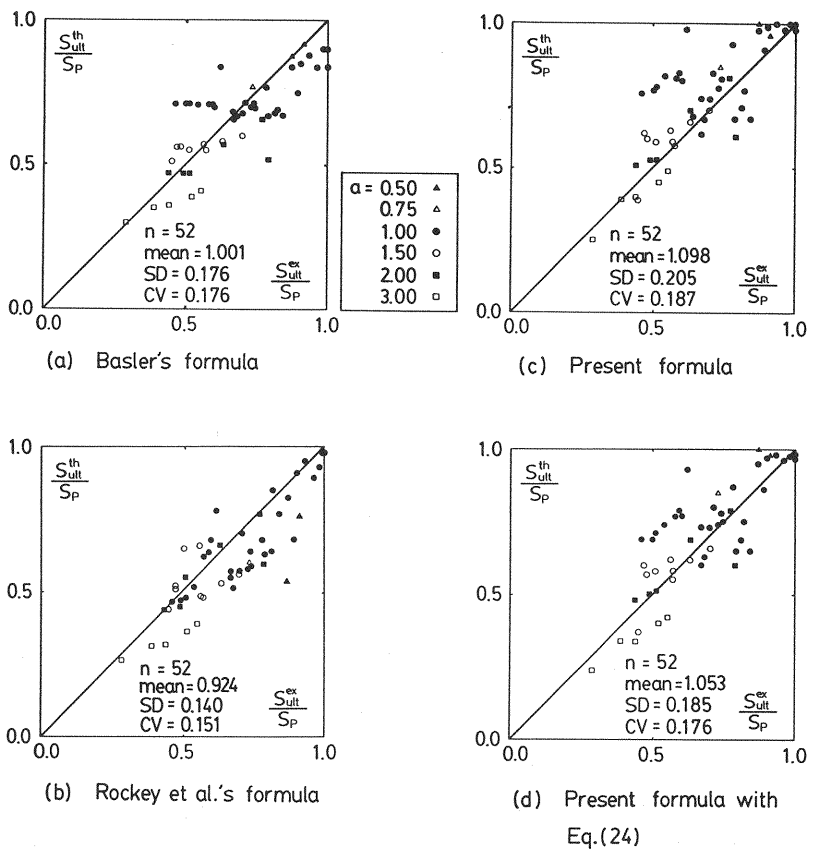

Fig. 12 Correlation of estimated ultimate shear strength by several formulae proposed with the available experimental results.

strength to the experimental one, the standard deviation and the coefficient of variation, respectively. Basler's formula represented in Fig. 12(a) gives the most correlative average value with the experimental ones. Although the formula of Rockey et al. in Fig. 12(b) gives lower strength than the experimental ones on an average, it shows the narrow variation.

The original formula presented here in Fig. 12(c) tends to estimate a little higher strength, especially in the range of the high ultimate strength. The reason for this is that these experiments have been carried out on the specimens which consist of several panels, and that the influence of the bending moment on the shear strength can not neglected. Therefore, when the modification in the previous article to take the bending moment into account is employed, the reduced shear buckling strength leads to the results in Fig. 12(d), where *mean*=1.053, SD=0.185, CV=0.176, and can give the closer correlative strength and the narrower variation. Note that the reduction of the buckling strength is not applied to the experimental cases[19] denoted by "G6" and "G7" Series by Basler, because these were carried out in primary shear. Since this is rather a rough modification to include the effect of the bending moment in the underestimated side, it is expected to consider the coupled strength more accurately.

5. CONCLUSION

The numerical simulation of the stress state in the tension field of a shear panel of plate girders is utilized to construct a stress distribution model in the ultimate state. On the basis of very simple assumptions of the stress field, a formula is proposed to predict the ultimate strength of a shear panel. This formula is compared with Basler's, and the correlation analysis of the proposed formulae including the present formula with available experimental results is carried out. The conclusions obtained are summarized as follows:

(1) The stress distribution is assumed in a simple form to express the ultimate strength in terms of only the shear buckling stress. Although our stress distribution model becomes the same as that by Marsh in the square web plate, the formula can apply in the wide range of mechanical parameters such as aspect ratio and depth-thickness ratio, because the estimation of the shear buckling strength is improved to take account of the contribution of the flange rigidity.

(2) Two types of relations between $(\sigma_c)_{\min}$ and α using linear and trigonometric functions are compared as an illustration to show that the choice of such a relation yields very small difference in the range of $0.6 \leqq \alpha \leqq 1.5$. The latter gives the simpler expression for the ultimate shear strength, and is proposed here as a better formula from the practical point of view. The formula also depends on the location where the total shear force is defined, and the largest difference occurs between the left- or right-most vertical surface and the mid-section of the panel. The present formula gives always conservative estimation than the one at the mid-section. Although the maximum difference becomes up to about 30%, this is caused by the fact that this model overestimates the shear stress level than those derived from the numerical analysis.

(3) Basler's model yields the smaller inclination of the tensile principal direction at the center of a panel than the one by the numerical analysis, which is smaller than that of the diagonal of a panel and becomes the smallest at the center of the panel. The angle ϕ presented here can explicitly include the effect of not only aspect ratio α and depth-thickness ratio β but also flange rigidity, and can reflect the numerical results fairly well.

(4) The estimated shear strength by our formula correlates closer with the numerical results. This formula tends to yield higher strength than the experiments and other formulae, because the reduction of the shear buckling strength due to the bending moment is not avoidable in the experiments. Therefore, the simple calculation to take into account the effect of the bending moment improves this tendency to give the closer correlative strength and the narrower variation. However, such an improvement simply may give an underestimated approximation of the actual interactive strength between shear and bending moment in the

case of the intermediate shear panels. Concerning to this coupled strength, the further investigation must be required.

6. ACKNOWLEDGEMENT

This study was supported in part by the Grant-in-Aid for Encouragement of Young Scientists from the Japanese Ministry of Education, Science and Culture.

REFERENCES

1) Basler, K. : Strength of plate girders in shear, Proc. ASCE, Vol. 87, No. ST 7, pp. 151-180, 1961.
2) Gaylord, E. H. : Discussion on 'Strength of plate girders in shear', Proc. ASCE, Vol. 88, No. ST 2, pp. 151-154, 1962.
3) Fujii, T. : On an improved theory for Dr. Basler's theory, Final Report, 8 th Congress, IABSE, New York, pp. 479-487, 1968.
4) Hasegawa, A., Nishino, F. and Okumura, T. : Ultimate strength of longitudinally stiffened plate girders in shear, Proc. JSCE, No. 235, pp. 13-28, 1975 (in Japanese).
5) Rockey, K. C. and Skaloud, M. : The ultimate load behavior of plate girders loaded in shear, The Structural Engineer, Vol. 50, No. 1, pp. 29-47, 1972.
6) Porter, D. M., Rockey, K. C. and Evans, H. R. : The collapse behavior of plate girders loaded in shear, The Structural Engineer, Vol. 53, No. 8, pp. 313-325, 1975.
7) Rockey, K. C., Evans, H. R. and Porter, D. M. : A design method for predicting the collapse behavior of plate girders, Proc. Institution of Civil Engineers, Vol. 65, Part 2, pp. 85-112, 1978.
8) Herzog, M. A. M. : Ultimate static strength of plate girders from tests, Proc. ASCE, Vol. 100, No. ST 5, pp. 849-864, 1974.
9) Moriwaki, Y. and Fujino, M. : Experimental study on shear strength of plate girders with initial imperfections, Proc. JSCE, No. 249, pp. 41-54, 1976 (in Japanese).
10) Niinobe, Y. : Study on the post-buckling strength of webplates of plate girders under shear, Proc. JSCE, No. 303, pp. 15-30, 1980 (in Japanese).
11) Cescotto, S., Maquoi, R. and Massonnet, Ch. : Simulation sur Ordinateur du comportement à la ruine des poutres à âme pleine cisaillées ou flechies, Construction Metallique, No. 2, pp. 27-40, 1981.
12) Marsh, S. : Theoretical model for collapse of shear webs, Proc. ASCE, Vol. 108, No. EM 5, pp. 819-832, 1982.
13) Kuranishi, S., Nakazawa, M. and Iwakuma, T. : On the tension field action and collapse mechanism of a panel under shear, Structural Eng./Earthquake Eng., Japan Society of Civil Engineers, Vol. 5, No. 1, pp. 161s-171s, 1988.
14) Dubas, P. and Gehri, E. : Behaviour and Design of Steel Plated Structures, Swiss Federal Institute of Technology, Zürich, pp. 110-111, 1986.
15) Budiansky, B. : Theory of buckling and post-buckling behavior of elastic structures, Advances in Appl. Mech., Vol. 14, pp. 1-65, 1974.
16) Timoshenko, S. P. and Gere, J. M. : Theory of Elastic Stability, 2 nd ed., p. 423, McGraw-Hill Book Co., New York, 1961.
17) Bleich, F. : Buckling Strength of Metal Structures, p. 407, McGraw-Hill Book Co., New York, 1952.
18) Edited by C. R. C. JAPAN : Handbook of Structural Stability, Part. Ⅲ, pp. 3-26, CORONA Publishing Co., Tokyo, 1971.
19) Hasegawa, A., Horiguchi, T. and Nishino, F. : A consideration on the load carrying capacity of plate girders (Part 2), Bridge and Foundation Engineering, Vol. 11, No. 5, pp. 8-12, 1977 (in Japanese).

(Received August 23 1988)